Material transformation studies with full-field measurements

André Chrysochoos

MATERIAL TRANSFORMATION STUDIES WITH FULL-FIELD THERMAL AND DEFORMATION MEASUREMENTS

A. Chrysochoos
Mechanical and Civil Engineering Laboratory, Montpellier II University
CC048, Université Montpellier II, Pl. E. Bataillon, 34095 Montpellier, France
chryso@lmgc.univ-montp2.fr

1. INTRODUCTION

Optical techniques associated with quantitative imaging methods have been developed considerably over the last twenty years. During a deformation process, these techniques enable us to obtain *discrete field measurements,* invaluable not only to characterize and identify material behaviors but also for better distinguishing "*material*" effects from *"structure"* effects at an observation scale imposed by the optical systems. For example, digital image correlation (DIC) gives access to kinematical data and allows considering the homogeneous character of deformation fields; infrared thermography provides temperature fields and gives information about the dissipative nature of deformation mechanisms (viscosity, plasticity, damage, etc.). It also enables us to show the existence of heat coupling sources which translate a strong interaction between thermal and mechanical states (thermodilatability, first order phase change, rubber effects, etc.).
Through this presentation, we wish to show that, parallel to theoretical and numerical work concerning *the multiscale* analysis of material behavior, it may be interesting and complementary to combine quantitative imaging techniques. During the presentation, we will briefly recall the definition of the different heat sources and the form of the energy balance associated with the deformation process; then, we will evoke the main characteristics of the experimental setup and that of the electronic synchronization system linking visible with infrared cameras; finally, we will seek to illustrate the potentialities of the combined imaging approach through results extracted from many applications: hardening and damage effects in metals, strain localization in polymers, phase change front tracking in SMAs, etc.. We will emphasize the role of the space observation scale in the definition of some behavioural properties of the material.

2. HEAT SOURCES AND ENERGY BALANCE

From a thermomechanical standpoint, deformation process is considered as a dissipative quasi-static process. The equilibrium state of each volume material element is then described using a set of N state variables: the absolute temperature T, a strain tensor ε and an N-2 element vector α which pools the so-called internal variables describing the macroscopic effects of complex, coupled microstructural phenomena. The rate of deformation energy is classically defined by $w_{\text{def}}^{\bullet} = \sigma : D$, where σ is the Cauchy stress tensor and D the strain rate tensor. The symbol $(\ )^{\bullet}$ signifies that the time variation of $(\ )$ is path-dependent. The local heat diffusion equation is written as:

$$\rho C\dot{T} - \text{div}(K\,\text{grad}T) = d_1 + s_{\text{the}} + s_{\text{ic}} + r_{\text{ext}} \tag{1}$$

where ρ is mass density, C the specific heat, K the conduction tensor. The heat sources are the intrinsic dissipation d_1, the thermomechanical coupling sources that pool the thermoelastic source s_{the} and the other internal coupling sources s_{ic} (e.g. latent heat rate), and the external volume heat supply r_{ext}. With the specific free energy $\psi(T,\varepsilon,\alpha)$, the volume heat sources d_1, s_{the} and s_{ic} are defined by:

$$\begin{cases} d_1 = \sigma : D - \rho\,\partial\psi/\partial\varepsilon.\dot{\varepsilon} - \rho\,\partial\psi/\partial\alpha.\dot{\alpha} \geq 0 \\ s_{\text{the}} + s_{\text{ic}} = \rho T\,\partial^2\psi/\partial T\partial\varepsilon : \dot{\varepsilon} + \rho T\,\partial^2\psi/\partial T\partial\alpha.\dot{\alpha} \end{cases} \tag{2}$$

3. EXPERIMENTAL SETUP

Figure 1 illustrates the experimental set-up designed for this purpose. It involves a MTS hydraulic testing machine (frame: 100 kN, load cell: 25 kN), a Cedip Jade III infrared camera and a Camelia 8M high resolution CCD camera. The optical axis of both cameras was set perpendicularly to the frame of the testing machine, and remained fixed during the test. A simultaneous record of infrared and visible images was performed on each side of the sample surface, and we therefore used thin, flat samples. Each camera was controlled by a separate computer. A specific electronic device was designed to synchronise the frame grabbing of the two cameras. Reference speckle and infrared images were mapped using a calibration target. Comparing the visible and infrared images of the target, we determined the rigid body movements and the scale factor ratios between the two cameras. For each acquisition time, the thermal data given by the IR camera (measured in the

current, Eulerian configuration) were linearly interpolated spatiotemporally using the positions of the deformed configuration given by the DIC computation.

Figure 1- Experimental setup

This operation allowed us to track the material surface element (*mse*) associated with the DIC mesh, and thus enabled us to compute and check the importance of the volume heat rate associated with the convective terms $\rho C \, \mathrm{grad}T.v$, where v is the velocity vector of *mse*.

4. EXAMPLE OF APPLICATION

Results extracted from an application example are shown here to give a brief overview of the presentation. The example given relates to the hardening and damage development during a monotonous straining of steel classically used in metal forming. The test was performed at constant velocity (0.25 mm.s^{-1}). Fig. 2a shows the time course of the longitudinal profile of the acceleration component in the loading direction, while Fig. 2b shows the corresponding evolution of the intrinsic dissipation profile.

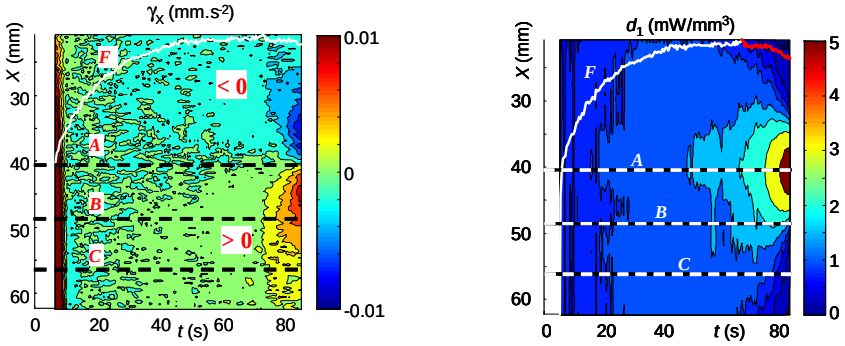

(*a*) (*b*)

Figure 2- Spatiotemporal variation in $\gamma_X(X,0,t)$ (*a*), and in $d_1(X,0,t)$ (*b*).

In the figures above, the horizontal axis represents the time while the vertical axis represents the longitudinal sample axis in the initial configuration. The load *vs.* time curve was superimposed in order to link the local data to the overall mechanical loading. The paths of three *mse* (***A***, ***B*** and ***C***) are plotted to illustrate the material flows. Element ***A*** is quite specific as it represents the fracture point. Elements ***B*** and ***C*** were *a posteriori* chosen to be respectively placed at the boundary and clearly outside the localization zone when the crack occurred. Naturally, as material particles remain fixed in the Lagrangian configuration, their paths are simple horizontal lines. Figure 2a shows that acceleration amplitude is negligible compared with the gravity acceleration ($\approx 10^{-5}$ m.s^{-2}). A steady concentration of level curves of positive and negative acceleration, distributed on both sides of the necking zones, is clearly observed. The section where the fracture will take place (*i.e*. *mse* ***A***) is then characterized by zero acceleration. Figure 2b presents the space-time distribution of intrinsic dissipation during strain hardening. Data processing was stopped before rapid growth of localized necking occurred to take into account only relatively small stress and strain-rate gradients and slight triaxiality effects (plane stress). The early narrowing of the level curves reveals a gradual development of localization, long before the maximum load is reached.

5. REFERENCES (*)

1. Chrysochoos, A., Louche, H., (2005), An infrared image processing to analyse the calorific effects accompanying strain localisation, *International Journal of Engineering Sciences,* 38, 1759-1788.
2. Wattrisse, B., Chrysochoos, A., Muracciole, J.-M., Nemoz-Gaillard, M., (2000), Analysis of strain localisation during tensile test by digital image correlation, J. of Experimental Mechanics, 41, 1, pp. 29-38.
3. Chrysochoos, A., Muracciole, J.-M., Wattrisse, B., (2000), Experimental analysis of strain and damage localization, *Proc Symposium on continuous damage and fracture*, Cachan, pp.41-51.

(*) related papers